

Abstract

Data recorded by the Ion Velocity Meter (IVM) as part of the Coupled Ion Neutral Dynamics Investigation (CINDI) aboard the Communication/Navigation Outage Forecasting System (C/NOFS) satellite are used to study equatorial plasma bubbles (EPBS) from 1600 to 0600 local time in altitudes from 350 to 850 km. The data are taken during the seven year period from 2008 to 2014, a period that spans more than one half of a magnetic Solar cycle and includes solar minimum and a moderate solar maximum. Here EPBS are identified by profiles in the plasma density using a rolling ball algorithm, and each has a depth measured as the percent change between the background density and the minimum density and a depth measured as the difference between the background density and the minimum density. We describe depletion parameters as a function of location and season with the goal to discover the relationships between these parameters and the generation and evolution of the depletions.

Introduction

- Atmospheric gravity waves and a collisional shear instability in the bottomside F region are both able to produce initial perturbations that can grow under the action of the Rayleigh Taylor instability [Hysell et al, 2005; Vadas & Fritts, 2004].
- When the duskside terminator aligns with the geomagnetic meridian, longitudinal gradient in Pedersen conductivity increases causing the growth rate for EPBS to rise rapidly after sunset making their detection more likely [Tsunoda, 1985], and produces an expected seasonal and longitudinal occurrence.
- Previous analysis of EPBS [Smith & Heelis, 2017] indicate a favored size near 200 km that is independent of solar activity.
- However the same study indicates that expected season, longitude and local time dependencies for EPBS are not well preserved at solar minimum.
- Here we examine the density profiles of EPBS observed in the topside ionosphere by the C/NOFS satellite with an objective of distinguishing characteristics that depend on solar activity changes that occur from 2008 to 2014.

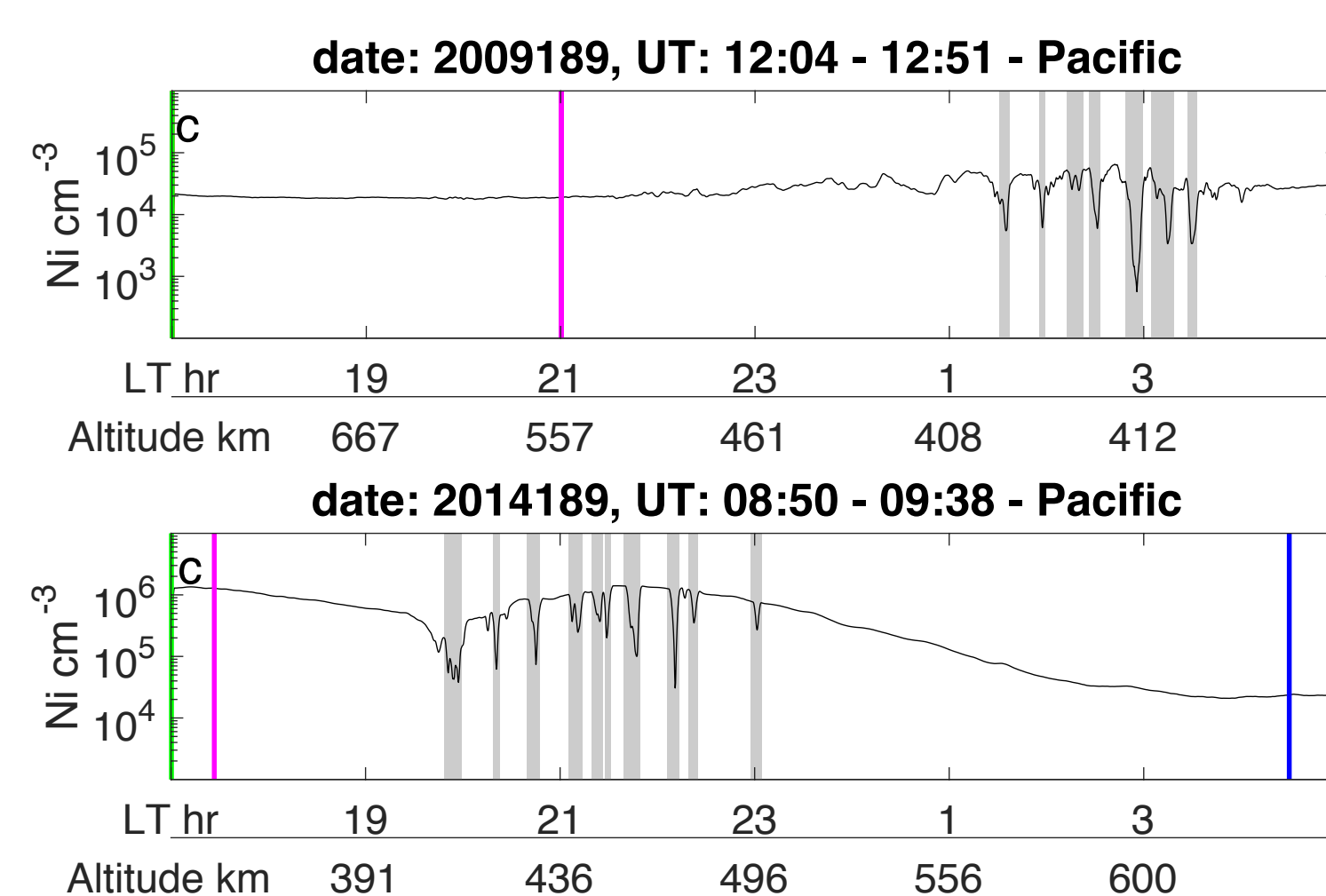


Figure 1. Two orbits are shown here. The top panel shows an orbit observed in 2009 and shows bubbles in the postmidnight sector. The bottom panel shows an orbit observed during 2014 with bubbles in the postsunset sector. These orbits show the difference in typical depth and local time distribution in solar minimum and solar maximum.

Method

- Coupled Ion Neutral Density Investigation (CINDI) data from the IVM on C/NOFS satellite between altitudes of 365 to 850 km are used.
- The pysat package for python is used for all handling of the CINDI data.
- Looking for depletions with scale sizes >100km. A median filter of the ion density over ~50km is taken to remove features below the scale size of interest.
- Delaunay triangulation is applied to filtered data, yielding a matrix of triangular simplexes.
- Triangles below the density profile and triangles with circumradii less than 9 seconds are removed.
- From these triangles, noncontiguous triangles are removed.
- The points belonging to vertices of the remaining triangles represent the background for the density profile.
- Adjacent points in the background that meet a minimum depth of .15 $\Delta Ni/Ni$ and a width to depth ratio greater than .15 $\Delta Ni/Ni$ are labeled as the leading and trailing edges of discrete bubbles. Bubbles with background densities below $1e03 \text{ cm}^{-3}$ are ignored due to the limitations of the instrument.
- In this initial study we examine the following key parameters for depletion regions observed in the nighttime sky from 1600 to 0600 within $\pm 10^\circ$ magnetic latitude and $\pm 13^\circ$ geographic latitude: local time, date, and depth.

Results

Rolling ball algorithm has the capability to identify discrete bubbles while simultaneously identifying a background density profile

LOW SOLAR ACTIVITY (~F10.7 = 70 s.f.u.)

Background density declines from $5e04$ - $5e05$ at 1800 to $1e03$ - $1e04$ 0300

ΔNi has a nearly identical decline as the background density

Largest $\Delta Ni/Ni$ bubbles seen in post midnight sector

MODERATE SOLAR ACTIVITY (~F10.7 = 130 s.f.u.)

Background density declines from $1e04$ - $1e06$ at 1800 to $5e03$ - $5e05$ at 0300

ΔNi has steeper decline than the background density

Largest $\Delta Ni/Ni$ bubbles seen in post sunset sector

The relationship between the background density and ΔNi determines to some extent $\Delta Ni/Ni$

Similar slopes between ΔNi and the background density produces a nearly uniform $\Delta Ni/Ni$ distribution in local time during 2009

A steeper decline in ΔNi than background density produces an asymmetrical $\Delta Ni/Ni$ distribution in local time during 2012

Shallowest bubbles seen at later local times for all solar activity levels

Bubbles of all depths are seen at all apex heights from 400 to 600 km.

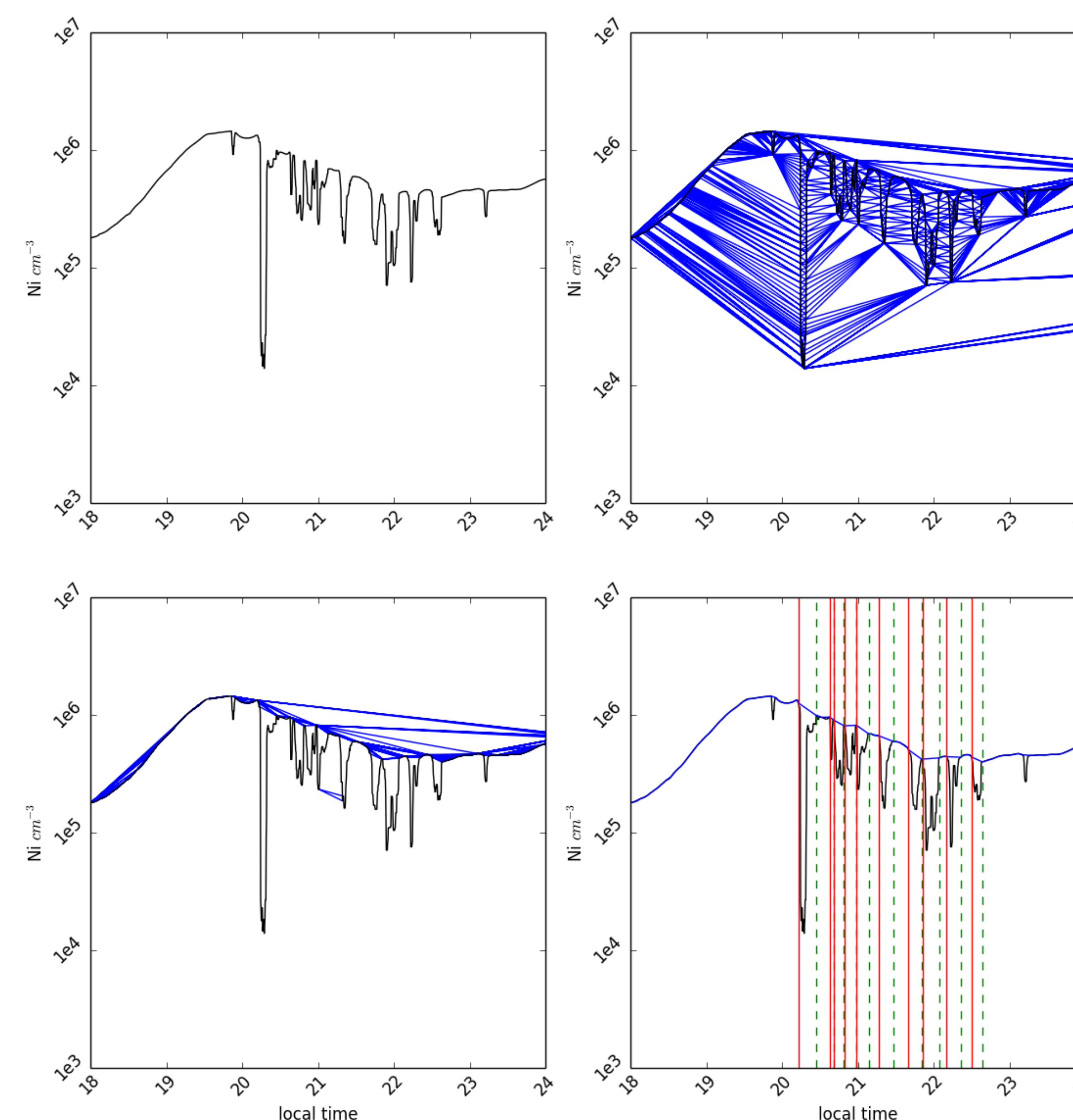
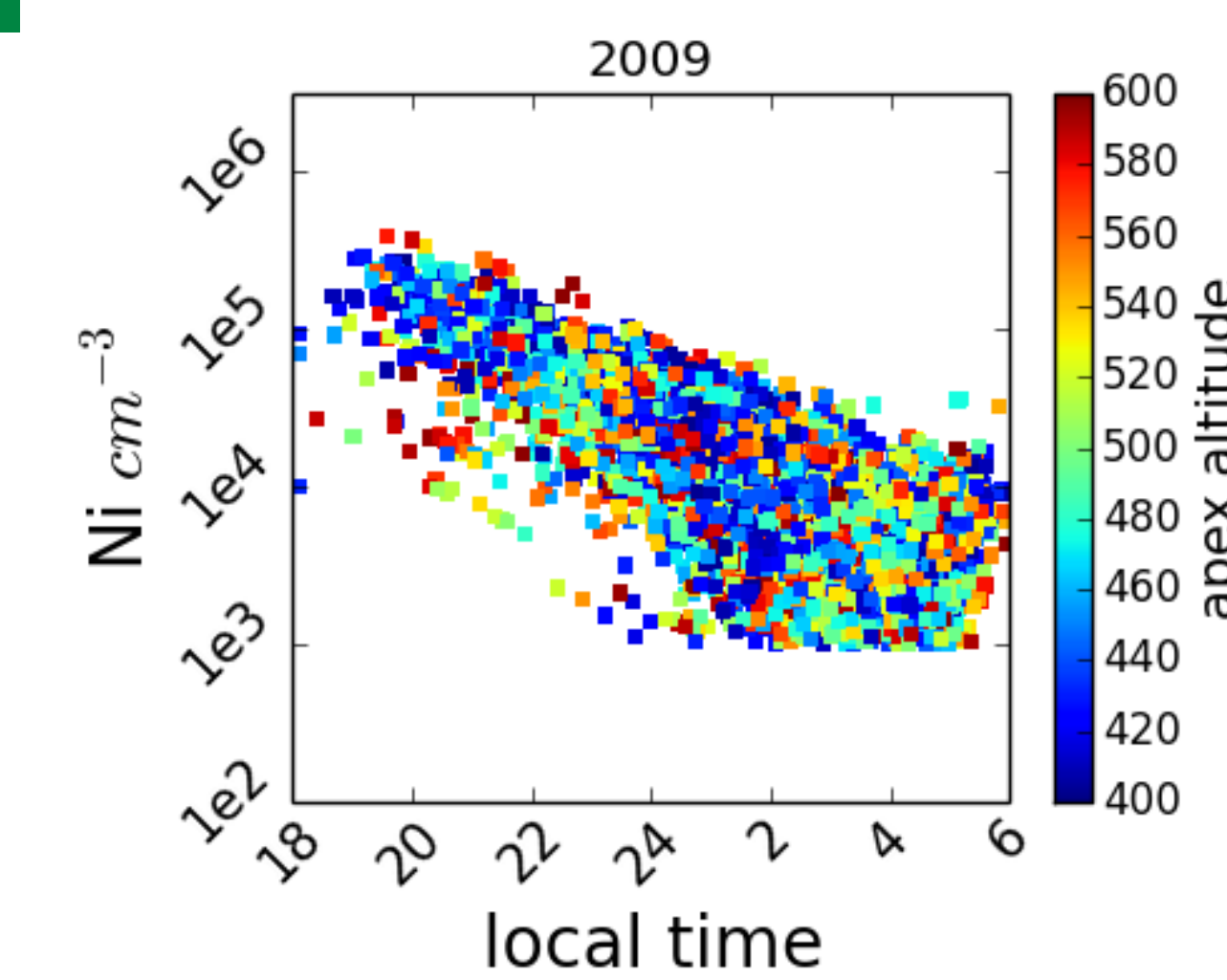


Figure 2. The process for locating plasma bubbles is shown here. The plots have been cropped to only show 1800 to 2400 since there are no post midnight bubbles during this orbit. The filtered density profile is shown in the top left panel. The density profile (black) and the Delaunay triangulation (blue) are shown in the top right panel. Triangles meeting selection conditions are shown in the bottom left. The bottom right panel shows the resulting identification of several plasma bubbles during this orbit with leading (red) and trailing (green) edges shown.

Low Solar Activity



Moderate Solar Activity

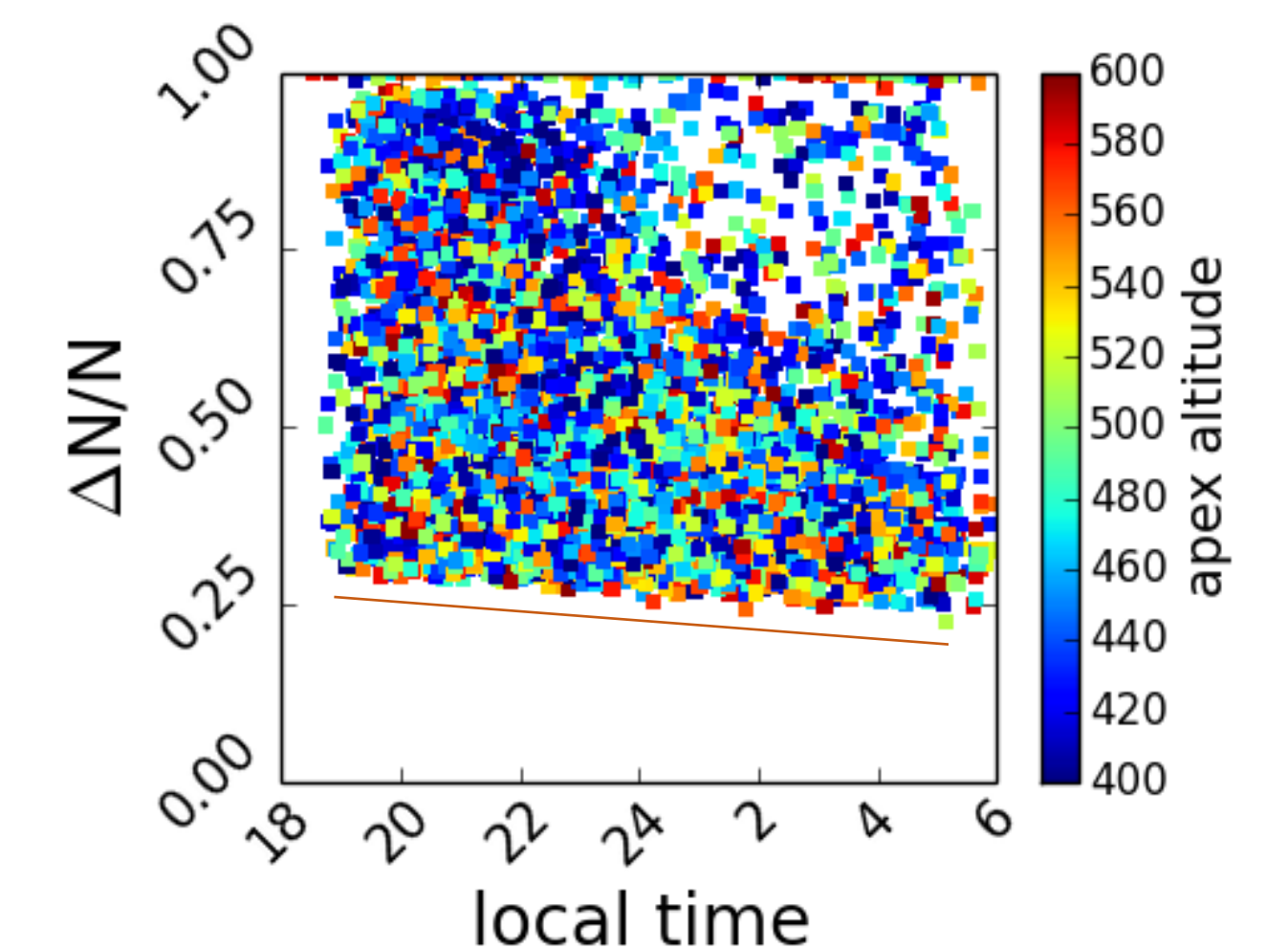
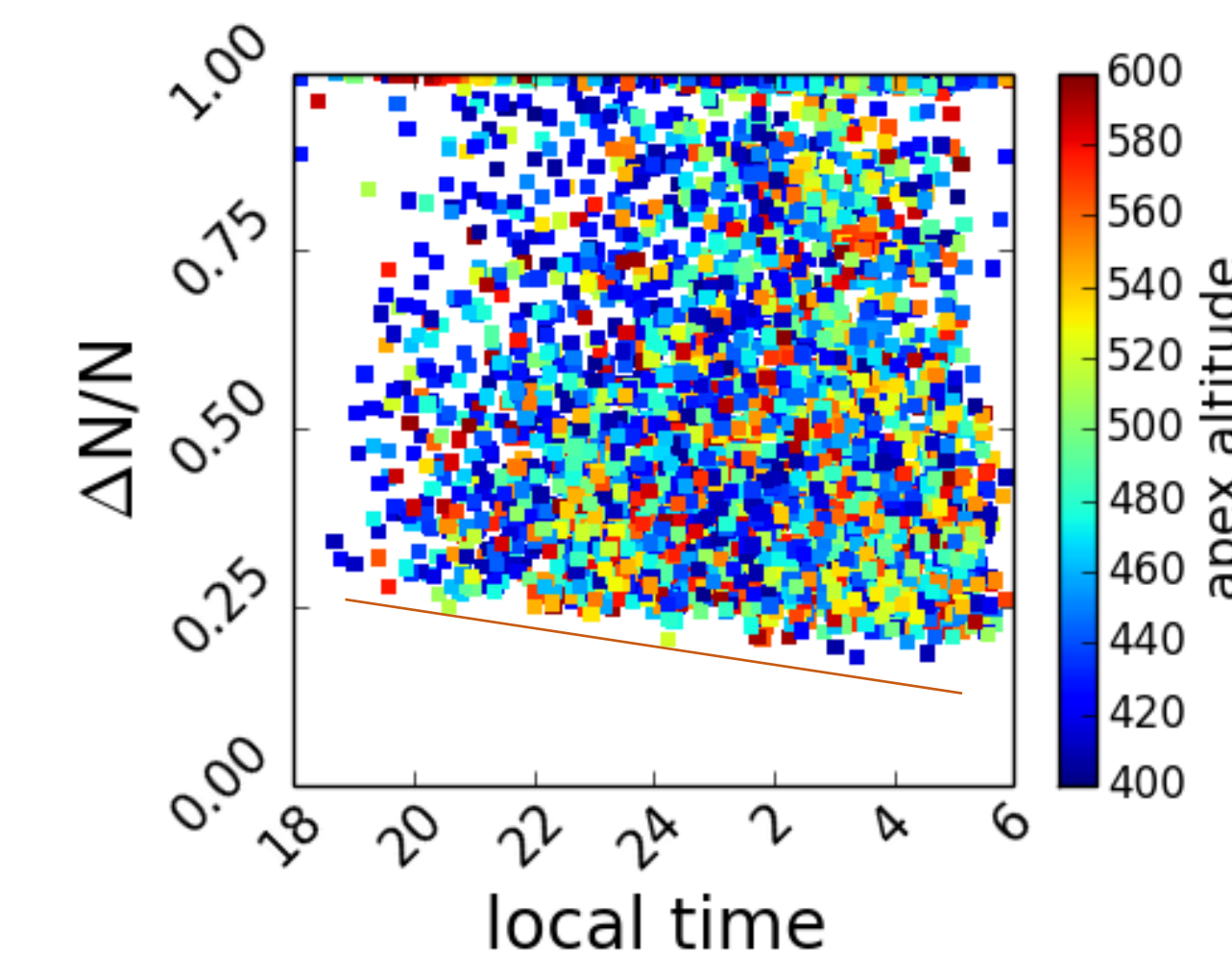
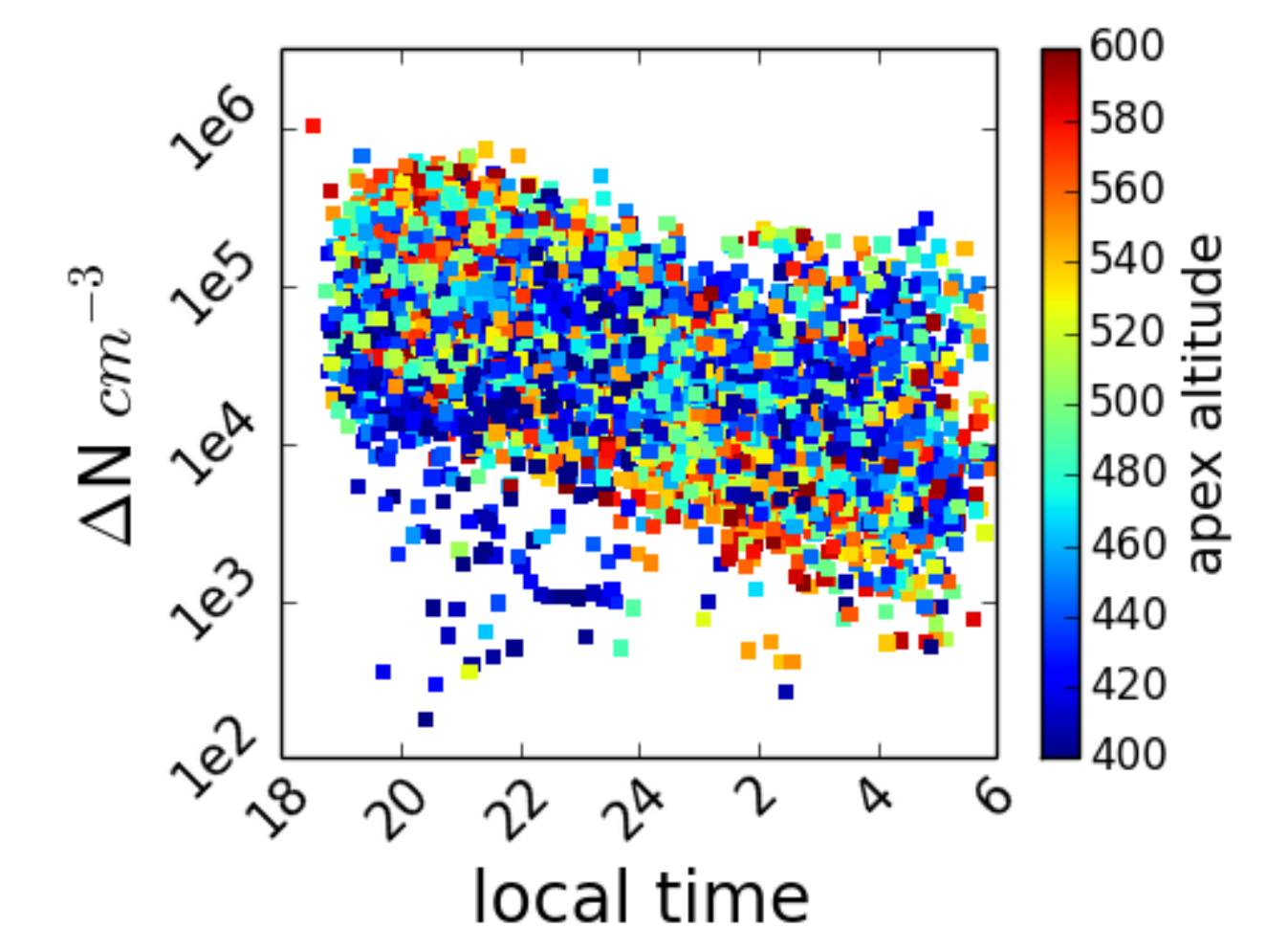
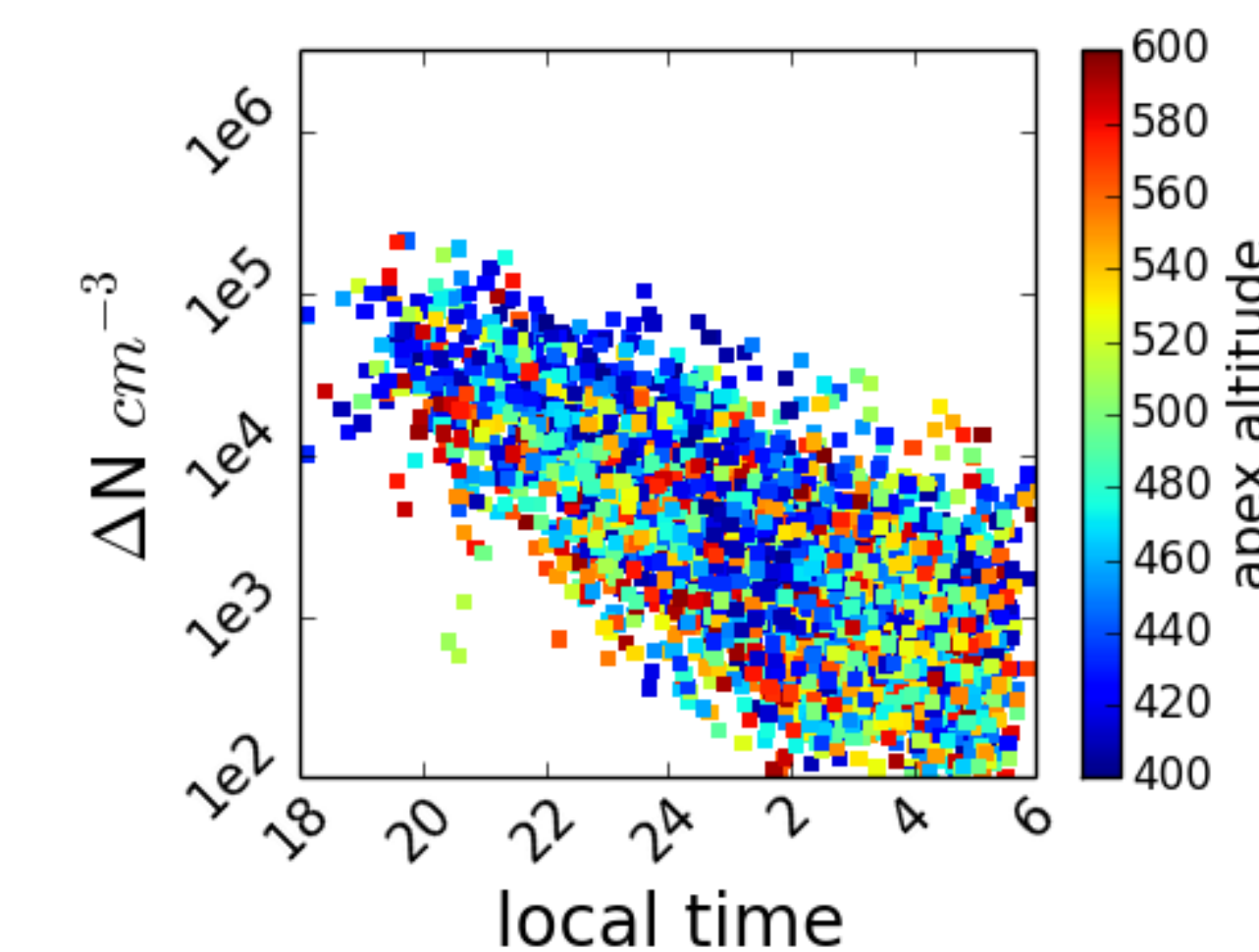
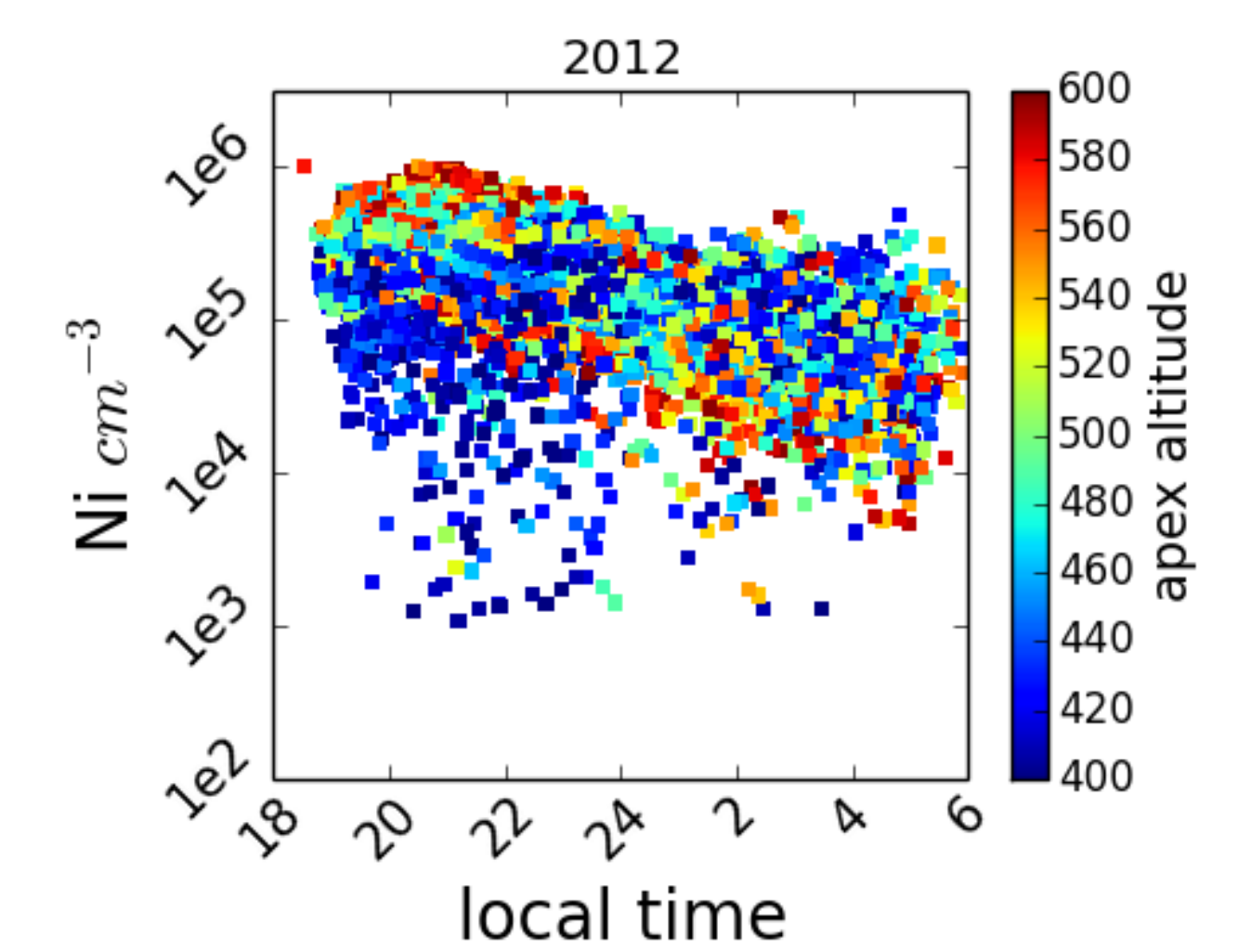


Figure 3. The distributions of (from top to bottom) bubble background densities, ΔNi , and $\Delta Ni/Ni$ in local time and apex longitude during two different solar activity periods is shown here. Each panel shows the distribution of bubble depths in local time, where each square's color indicates the apex altitude of that bubble. The left panel shows this distributions for bubbles observed during 2009. The right panel shows this distributions for 2012.

Conclusions

- Background density profiles are drastically different in local time, with a much steeper decline in background density occurring over the local time region in low solar activity than moderate solar activity.
- EPB ΔNi are distributed similarly to the background density with discrepancies in slope producing different $\Delta Ni/Ni$ distributions
- EPB $\Delta Ni/Ni$ are distributed very differently in local time under different solar activity conditions but appear to have no dependence on apex altitude.
- Large $\Delta Ni/Ni$ bubbles observed in the post sunset period during moderate solar activity period are identified as newly evolved features from the bottomside
- Fewer such features at low solar activity indicates that EPBS do not rise through the F-peak during this period
- Large $\Delta Ni/Ni$ bubbles observed in the post midnight period during low solar activity period are identified as newly evolved features from the bottomside.
- Fewer such features at moderate solar activity indicates that EPBS are created more frequently in the post-midnight sector at low solar activity.

References

- Hysell, D. L., E. Kudeki, and J. L. Chau. "Possible ionospheric preconditioning by shear flow leading to equatorial spread F." *Annales Geophysicae*. Vol. 23. No. 7. 2005.
- Smith, J., and R. A. Heelis (2017), Equatorial plasma bubbles: Variations of occurrence and spatial scale in local time, longitude, season, and solar activity, *J. Geophys. Res. Space Physics*, 122, doi:10.1002/2017JA024128.
- Tsunoda, Ronald T. "Control of the seasonal and longitudinal occurrence of equatorial scintillations by the longitudinal gradient in integrated E region Pedersen conductivity." *Journal of Geophysical Research: Space Physics* 90.A1 (1985): 447-456.
- Vadas, Sharon L., and David C. Fritts. "Thermospheric responses to gravity waves arising from mesoscale convective complexes." *Journal of atmospheric and solar-terrestrial physics* 66.6 (2004): 781-804.